General Information

Date Written/Revised	02/12/2011
Title	In-situ and laboratory based out-of-plane testing of unreinforced masonry walls strengthened using near surface mounted twisted steel bars (138 Characters)
Submitted to	Journal of Construction and Building Materials
Authors	**Name:** Najif Ismail **Qualification:** M.E., B.E. (Hons) **Position:** Ph.D. Student **Organisation:** University of Auckland, New Zealand. **Address:** Department of Civil & Environmental Engineering University of Auckland, Private Bag 92019, Auckland 1142, New Zealand. **E-mail:** nism009@aucklanduni.ac.nz **Tel:** +64212166562
	Co-author **Name:** Jason M. Ingham **Qualification:** Ph.D., M.E. (Dist), MBA, B.E. (Hons) **Position:** Deputy Head of Department (Research) **Organisation:** University of Auckland, New Zealand.
Word Count	4172 (excluding references and abstract); Number of references = 23
No. of Tables	4
No. of Figures	11
Highlights	NSM bonding of TS bars used for strengthening the test walls Full scale cyclic out-of-plane testing of strengthened walls performed Numerous seismic response parameters investigated and reported The flexural strength increase ranged between 143% to 434% Strengthened walls exhibited highly ductile response

Abstract

The out-of-plane behaviour of unreinforced masonry (URM) walls strengthened using near surface mounting of twisted steel bars (NSM-TS) was investigated by performing two series of tests, which involved in-situ and laboratory based out-of-plane testing of full scale strengthened URM walls. In the first series of testing, two walls were strengthened and tested in-situ inside an historic URM house located in Wellington (New Zealand), known to be originally constructed in 1884 and to have undergone several minor periodic alterations. In the second series of testing, the results of in-situ testing were further confirmed by performing laboratory based reverse cyclic out-of-plane testing of two slender URM walls that were constructed using vintage solid clay bricks and a low strength hydraulic mortar, replicating typical historic URM construction. Numerous parameters pertaining to the out-of-plane behaviour of NSM-TS strengthened URM walls were investigated, including failure modes, hysteretic response curves, out-of-plane flexural strength, maximum drift, pseudo-ductility, and strain distribution in the NSM-TS bars. Finally, measured performance parameters from the strengthened walls were compared to the corresponding data from the as-built tested walls. It was inferred from the results that the observed flexural strength increase due to NSM-TS strengthening ranged from 143% to 434% when compared to the strength of as-built URM wall.

Keywords

In-situ testing; seismic strengthening; out-of-plane; unreinforced masonry; near surface mounting; steel bars.

1. Introduction

Unreinforced masonry (URM) bearing wall buildings in New Zealand were mostly constructed between 1880 and 1930 and being amongst the oldest buildings of the country constitute a significant portion of the country's architectural heritage [1], but the majority of these historic URM buildings are potentially prone to collapse in a moderate to large magnitude earthquake and pose a considerable safety hazard to their occupants. Many instances of URM buildings performing inadequately were observed during the recent 2010/2011 Canterbury (New Zealand) earthquake sequence [1-4], illustrating the seismic risk associated with this building type.

A number of seismic strengthening techniques have been implemented in the past to improve the seismic performance of URM buildings. Amongst such typical applications are the introduction of secondary lateral load resisting frames (steel or concrete), steel reinforced and polymer fibre reinforced shotcreting, diaphragm stiffening, unbonded posttensioning, insertion of steel bars into cored circular cavities located at the centreline of the wall, surface bonding of epoxy impregnated glass fibre reinforced polymer sheets, surface overlay of polymer textile reinforced mortars, and base isolation. A relatively new strengthening technique is the near surface insertion/mounting of high strength twisted steel bars (NSM-TS), in which thin slots are cut into the surface of the masonry and the twisted steel (TS) bars are bonded into the slot using either an epoxy or a cementitious grout. The addition of TS bars in URM walls allows the strengthened wall to be designed and to perform as a reinforced masonry wall, where the additionally installed bars restrain the opening of cracks and increase the load carrying capacity and/or ductility of the wall.

Currently, NSM-TS is typically used for non-seismic repairing and strengthening applications

that involve NSM bonding of TS bars in mortar bed joints to create deep beams or lintels, stitching across existing cracks, structural tying between intersecting structural walls, and structural tying of veneers to backing walls. Photographs of a URM building being strengthened using NSM-TS are shown in Figure 1, where the (cavity wall) front façade of the URM building was strengthened by installing replacement cavity ties and NSM bonding of TS bars in mortar bed joints, to increase stability of the masonry and to improve the seismic performance of the building.

The NSM-TS technique is claimed to have numerous advantages, with some of these briefly discussed herein. The NSM-TS technique involves minimal disruption to building function and only minor architectural alteration, which is deemed advantageous for buildings having an exposed brick masonry facade. The application does not increase the seismic weight of the structure and thus requires no additional foundation improvements.

1.1. Past testing

The use of TS bars to strengthen URM walls dates back to the early 1980s, when the technique was mainly used for the rehabilitation of cavity walls that involved installation of replacement ties between the outer veneer and the backing wall. Research investigating the suitability of NSM-TS for rehabilitation and repair of buildings progressed at a slow rate, with experimental studies mostly focusing on the flexural behaviour of masonry deep beams supporting gravity loading. One such experimental program was undertaken by Stepanek and Czempiel [5] that involved pull out testing and flexural testing of 18 NSM-TS strengthened laboratory built clay brick masonry beams, each being 600 mm deep and 2700 mm long. The test beams were either 250 mm wide (referred to as type A) or 380 mm wide (referred to as type B). The study concluded that an embedment length of 300 mm provided sufficient anchorage to cause the tensile yielding of a 6 mm twisted steel bar, being similar to the

results of pull out testing reported by Ismail et al. [6]. The flexural strength increase for type A beams was 124% when TS bars were installed on one face and 143% when TS bars were installed on both faces, whereas the increase in the flexural strength of type B beams for single sided and double sided application was observed to be 181% and 233% respectively. Moreover, the performance of URM arch bridges and masonry vault structures strengthened using a similar bar-grout system has also been extensively investigated [7-9].

Several precedent experimental programs have investigated the out-of-plane behaviour of clay brick masonry walls strengthened using NSM bonding of polymeric strips/bars [10, 11]. Italian researchers used NSM bonding of deformed steel bars in mortar bed joints to avoid masonry strength degradation resulting from creep deformation [12, 13], which is a typical strengthening intervention for heritage URM buildings located in non-seismic European countries. In a relatively recent research study, the effectiveness of NSM-TS for seismic strengthening of historic clay brick masonry walls was investigated by performing induced diagonal shear testing of strengthened masonry assemblages [6]. This study reported NSM-TS as a potentially viable seismic strengthening technique for in-plane loaded historic URM walls.

1.2. Strengthening procedure

For NSM-TS strengthening of URM walls, at the onset the masonry substrate surface is prepared by grinding any surface undulations and removing dust, paint, oil and/or any loose masonry fragments. Thin surface slots (being 30 mm deep and 4 mm wider than the outer bar diameter) are cut into the masonry surface using a hand held wet circular masonry saw that typically required two closely spaced cuts and removal of the masonry strip formed between these two cuts using a chisel. Additionally, commercially available wet masonry saws can be mounted with an adjustable guide to maintain the depth and alignment of cutting. To reduce

the amount of brick cutting, straight slots may be positioned to pass through a maximum number of mortar head joints. This cutting strategy was adopted for the strengthened walls reported herein, and was found to provide adequate bar anchorage. The cut slots are cleaned with an air blower or flushed with water and are left to dry until a saturated surface dry condition is reached. A water based primer can also be sprayed in the slots by using a blow pump to avoid moisture movement between the injected grout and the substrate masonry.

An approximately 10 mm thick bead of grout is injected into the back of the slot using a hand held injection gun. The twisted steel reinforcing bars are inserted into the slot by pushing the bars with a finger trowel into the injected bead of grout, and the slot is filled with grout. The slot is concealed by re-pointing using a tinted hydraulic mortar to match the existing masonry bond pattern. Figure 2 show a typical NSM-TS section and photographs illustrating the strengthening procedure.

2. Material properties

Series 1 testing was conducted on in-situ walls located inside a residential house (hereafter referred to as Avon House) situated at 44 Wallace Street Mt. Cook, Wellington, New Zealand. Avon house was originally constructed in 1884 and has undergone several minor periodic alterations, including the construction of a new retaining wall on the southwest side of the building. The load bearing URM walls consisted of handmade clay bricks, being on average 68 mm × 112 mm × 210 mm in size, and a low strength hydraulic masonry mortar. The walls had a rendering coat of 10-26 mm thick plaster on both the interior and the exterior faces. The bond pattern of the two leaf thick brick masonry wall was inconsistent, with a relatively small number of header courses interconnecting the two leafs together.

Masonry material properties for the in-situ tested walls (series 1) were determined and

reported by Lumantarana [14], and are reproduced in Table 1 for completeness. Series 2 test walls were constructed using vintage solid clay bricks and a low strength hydraulic mortar having a volumetric mix ratio of 1:2:9 (cement:lime:sand). The vintage clay bricks were 75 mm × 110 mm × 220 mm in size and were salvaged from the rubble of a roughly 104 years old historic URM building. Several standardised material tests were performed for establishing masonry material properties of series 2 test walls. Masonry flexural bond strength was determined by performing in-situ and laboratory based bond wrench tests in accordance with ASTM C1072-10 [15]. The brick flexural strength was determined in accordance with AS/NZS 4456-03 [16] and mortar compressive strength was determined in accordance with ASTM C109-11 [17]. The compressive strength of bricks and masonry were determined in accordance with ASTM C67-11 [18] and ASTM C1314-11 [19] respectively. Masonry diagonal shear strength was determined in accordance with ASTM E519-10 [20]. The results of masonry material testing are reported in Table 1 as mean values and corresponding coefficients of variation (COV).

For strengthening the test walls, a commercially available improved bar-grout system was used that consisted of high strength austenitic stainless steel (ASTM Grade 316) reinforcement bars (cold formed and twisted into a helical profile) and a two component based high bond strength non-shrink thixotropic injectable cementitious grout. The grout used is deemed to be compatible with porous heritage masonry and to have high fire resistance, but no experimental data has been found to support this claim. The helical profile along with the high strength allows self drilling of replacement veneer ties without disrupting the building function. Additionally, the stainless steel bars are not susceptible to corrosion/rusting, can readily be bent/hooked if additional anchorage is required, have higher fire resistance than do normal deformed steel bars and the helical profile of the twisted steel bars results in excellent mechanical anchorage over short bond lengths. The indicative physical characteristics of the

TS bars and the injection grout are reported in Table 2. It should also be noted that the TS bars exhibit prolonged strain hardening and continue to resist the same magnitude of tensile stress up to a strain value of approximately 0.03 mm/mm. Figure 3a shows a photograph of the TS bar and Figure 3b shows representative experimental stress-strain curves of the TS bars.

3. Experimental program

The testing program involved cyclic out-of-plane flexural testing of four slender URM walls, which was performed in two series of tests. The test walls were strengthened using either one 10 mm or two 6 mm vertically oriented NSM-TS bars. As the testing reported herein was used as a proof of concept for a relatively new technology, rather than as an optimised design assessment, manufacturer recommended reinforcement patterns were used for strengthening the test walls. The strengthened walls were then subjected to a uniformly distributed cyclic face loading and the effectiveness of NSM-TS as a seismic strengthening technique was established. Test walls were given the notation ABO-N or TSO-N, where AB refers to as-built tested walls, TS refers to walls strengthened using NSM-TS, O refers to out-of-plane testing and N denotes the test number. Test wall specifications and strengthening details are shown in Table 3.

In series 1 testing, two URM walls were strengthened using NSM-TS and were tested in-situ as a part of a large field testing program that involved masonry material testing, in-plane testing of as-built URM wallettes, out-of-plane testing of as-built slender URM walls and out-of-plane testing of URM walls strengthened using NSM-TS and NSM bonding of carbon fibre reinforced polymer strips. The out-of-plane behaviour of as-built URM walls was reported by Derakhashan [21] and the results are reproduced herein for comparison. Figure 4a shows a photograph of Avon house and Figure 4b shows the location of the test walls inside

the building.

Series 2 testing involved laboratory based reversed cyclic out-of-plane testing of two full scale slender URM walls, with one test wall strengthened using NSM-TS and the other wall tested as-built for comparison. Figure 5 shows the geometric dimensions of the test walls along with the orientation and the location of NSM-TS bars.

3.1. Testing details

For all test walls, a uniformly distributed cyclic face loading was applied by gradually inflating and deflating vinyl airbags that were capable of withstanding an air pressure of 15 kN/m^2. A gap of 80 mm was left between the wall and the backing frame that consisted of an assemblage of plywood sheets and steel angles. The backing frame was further supported horizontally with four 10 kN S-shape load cells that transferred applied lateral force to a rigid reaction frame. In order to ensure that the entire applied lateral force was transferred through the load cells, two pairs of smooth greased steel plates were placed underneath the plywood backing frame. The resulting lateral displacement occurring at wall midspan was measured using a linear variable differential transducer (LVDT) attached between the wall midspan and a free standing frame. The data from load cells and LVDTs was collected at 50 Hz using a 10 Volt excitation data acquisition system.

In order to simplify the in-situ testing (series 1) and to allow possible comparison to the concurrent series 2 testing of the laboratory-built walls, a 1200 mm long section of in-situ wall was isolated by making two vertical cuts through the in-situ walls using a concrete cutting chainsaw. The orientation of the vertical side cuts eliminated wedging effects after wall deformations had occurred. A reaction frame was constructed on site that consisted of vertical and diagonal timber members which were bolted to timber rails to transfer the horizontal load into the masonry wall located parallel to the wall being tested.

As the wall used for testing of ABO-2 and TSO-5 was scheduled for partial demolition up to a height of 2700 mm, the gravity load from the above remaining brickwork was temporarily supported by using equally spaced timber beams which were further supported by two temporary timber portal frames located on both sides of the wall. To provide horizontal restraint at the top of the test walls and to provide horizontal stability to the temporary portal frames, two diagonal timber members were connected between the top beam of the portal frame and the joists of the existing timber floor. Once the propping assembly was in place, the top of the test wall section was isolated from the main wall by gradual removal of masonry units until a clear gap of 50 mm was formed. The gap allowed the wall section to behave as a one-way spanning simply supported face loaded URM wall during the testing and prevented arching action from occurring. Figures 6a and 6b show the cross section of the two test setups used for in-situ testing.

The cross section of the test setup used for series 2 testing is shown in Figure 7. In series 2 testing, two backing frames were positioned on either side of the wall and a reversed cyclic face loading was applied by alternatively inflating the air bags positioned on either side of the wall. Additionally, a total of six 2 mm long strain gauges were directly attached to the NSM-TS bars that allowed the strain distribution to be monitored over their entire length. Figure 8 show photographs of the test walls ready to be tested.

3.2. Testing results

An overview of testing results is reported in Table 4. The experimentally measured maximum total applied lateral force V_u, together with the corresponding analogous moment M_u, are reported for each test wall, with the strength of each wall also expressed as a ratio with respect to the strength of the corresponding as-built wall. A first cracking limit state corresponding to the elastic limit of the test walls was considered to occur at an applied

lateral force of $0.7V_u$ where V_u is the maximum measured lateral force, being consistent with typical code recommendation for the elastic limit of a bi-linear idealisation [22, 23]. The ultimate strength limit state was defined as the point on the experimental force-displacement curves where wall strength degraded to 80% of the peak wall strength.

3.2.1. Failure modes

Figure 9 shows the damage patterns observed at the conclusion of testing. As-built walls behaved linearly until a single large crack developed at or near midspan and subsequently excessive mortar deterioration occurred at the crack location (Figure 10a). The cracking was mostly concentrated at mortar bed joints except in wall ABO-2, where the crack propagated through bricks (Figure 10b). The observed crack propagation through bricks was attributed to the presence of the strong cement based plaster (established by performing in-situ scratch tests) on the wall tension face and the relatively low brick strength. Upon further application of lateral loading, the upper and the lower portions of the walls started to rock about the crack location until the test was discontinued (prior to reaching a midspan instability displacement).

In all strengthened wall tests, opening of one or two large horizontal cracks in the upper one third portion of the wall and hairline cracking in the vicinity of NSM-TS bars was observed. Once the cracking initiated, the NSM-TS bars started to resist lateral wall deformations by restraining further opening of the cracks. At large displacements the grout used to install the NSM-TS bars around the crack location was observed to deteriorate due to excessive local bending of NSM-TS bars, with bar slippage not observed during any test. Residual displacements were observed after large displacement excursions in test wall TSO-5, which was partially attributed to local bending of the NSM-TS bar and partially to loose masonry fragments wedging into the vertical cuts made to isolate the wall section and engaging the remaining portion of the main wall. Figure 10c shows a photograph of one such exposed bent

NSM-TS bar at the crack location.

3.2.2. Force-displacement response

Figures 11b to 11d show experimentally measured hysteretic response for the test walls, with analogous moment and drift values shown on the secondary axes. The experimentally measured lateral force was transformed into analogous moment using Equation 1 and corresponding drift values were calculated using Equation 2, where Δ is the measured midspan displacement, V is corresponding total applied lateral force and H is the effective wall height. In order to illustrate the seismic improvement due to NSM-TS strengthening, the results for the corresponding as-built wall test (dotted lines) are also shown for each strengthened wall.

$$M = \frac{VH}{8} \quad (1)$$

$$\theta = \frac{2\Delta}{H} \quad (2)$$

In general, all as-built walls exhibited linear-elastic behaviour up to cracking and subsequently started to behave in a ductile rocking manner, with the wall first cracking strength depending upon the strength of constituent masonry materials and the residual strength of the cracked wall being dictated by wall geometry and the magnitude of overburden weight. Relatively large first cracking strength and sudden post-cracking strength degradation was observed for test wall ABO-2, which was attributed to the presence of the strong plaster on the wall tension face.

All strengthened walls exhibited a bi-linear behaviour, with post-cracking strength provided by the NSM-TS bars restraining further opening of the cracks. For wall TSO-4, it was observed that the NSM-TS repair not only increased the strength of the wall (434% when compared to the strength of cracked wall ABO-1) but also caused the wall to respond in a

highly ductile manner.

Test wall TSO-5 performed similarly to the as-built wall ABO-2 until cracking occurred but then exhibited large flexural strength (143% when compared to the strength of ABO-2), without any strength degradation. Small lateral displacement of the wall restraint at the top end of the wall was also observed to occur, which could have decreased the tensile stress in NSM-TS bar and thus resulted in lower flexural strength than that of a properly restrained NSM-TS strengthened URM wall. A more noticeable bi-linear behaviour was observed for test wall TSO-6, with the wall exhibiting a large flexural strength (300% when compared to the strength of ABO-3) when the strengthened face of the wall acted in tension, but the wall exhibited a relatively smaller strength gain (125% when compared to the strength of ABO-3) in the reverse direction when the NSM-TS bars acted in compression.

3.2.3. Ultimate drift and ductility

The ability of a laterally loaded structural member or assemblage to undergo lateral deformation without collapsing is termed ductility, which is a characteristic that is crucial in order for strengthened walls to perform adequately and to allow ample time for evacuation in the event of a large earthquake. The ductility of strengthened walls was quantified using the measured ultimate drift ratio $\theta_u = \frac{2\Delta_u}{H}$ and a pseudo-ductility value $\mu = \frac{\Delta_u}{\Delta_y}$, where Δ_y is the effective yield displacement corresponding to extrapolation of the first cracking limit state when considering a bi-linear elasto-plastic system (refer Figure 11a), Δ_u is the midspan displacement corresponding to the ultimate strength limit state and H is the effective wall height.

The behaviour of as-built tested walls ABO-1 and ABO-3 in terms of ductility was similar to that typical for face loaded one way spanning out-of-plane loaded URM walls, with the walls

continuing to resist forces even at large wall drift. However, wall ABO-2 performed differently and exhibited sudden strength degradation after cracking. None of the strengthened walls reached their ultimate strength limit state before the air bags reached their inflation capacity and the testing was discontinued, which was attributed to the large strain capacity of the TS bars.

3.2.4. Initial wall stiffness

Initial wall stiffness is of interest when considering the seismic behaviour of URM structures. The stiffness of test walls was quantified by the initial stiffness value K_i, which is defined as the slope of the initial linear limb (corresponding to elastic response of the walls) of the force-displacement curve. The initial wall stiffness was calculated as a chord modulus between two points, corresponding to lateral force values of $0.05V_u$ and $0.7V_u$, on the linear portion of the experimental force-displacement curves (refer Figure 11a). The determined initial stiffness values are reported in Table 4.

3.2.5. Tensile strain in TS bars

All six strain gauges monitored tensile strain occurring in the NSM-TS bars during the testing of wall TSO-6, with all strains observed to be negligibly small prior to wall cracking and subsequently observed to increase gradually as the testing proceeded. The stress distribution along the bar length further suggested that the bars restrained crack openings at several bed joint locations. A maximum tensile strain value of 0.013 mm/mm (analogous to a tensile stress of 1220 MPa) was recorded through strain gauge SG-4, being more than the strain analogous to 2% offset yield strength of the bar, whilst the tensile strain in the other bar at the same location (0.009 mm/mm and analogous to tensile stress of 980 MPa) did not reach the indicative yield strain (0.012 mm/mm). The observed difference of strain values was attributed to torsional twisting of the backing frame.

4. Summary and Conclusions

The history of research and development of the NSM-TS strengthening technique is first reported, with an emphasis on seismic repairing and strengthening of historic clay brick masonry buildings. A summary of precedent experimental programs is presented and an experimental program was undertaken to fill an identified gap in the current database of experimental results regarding the seismic performance of NSM-TS strengthened URM walls. The experimental program investigated the reversed cyclic out-of-plane performance of slender URM walls strengthened using NSM-TS bars through two series of full scale out-of-plane flexural testing of six (6) strengthened URM walls. The test boundary conditions represented actual wall boundary conditions in real buildings and in particular allowed determination of the relative effectiveness of NSM-TS to improve the out-of-plane flexural strength of URM walls spanning between two adjacent diaphragms. Numerous structural characteristics pertaining to the seismic behaviour of URM walls strengthened using NSM-TS were investigated and then compared to those obtained from the corresponding as-built wall. The key findings of the experimental program are:

- All strengthened walls exhibited a ductile bi-linear behaviour and did not reach an ultimate strength limit state before the testing was discontinued, which was attributed to the large strain capacity of the twisted stainless steel bars.

- It was established from the results of precedent experimental studies that short embedment lengths (roughly 300 mm) provided sufficient anchorage to cause tensile yielding of the TS bars, which was further confirmed in the testing reported herein.

- NSM-TS restrained further opening of flexural cracks by acting in tension and no bar slippage was observed during the testing, suggesting that the NSM-TS strengthened walls are conceptually similar to conventional reinforced masonry walls.

- NSM-TS repairing not only increased the strength of the cracked URM wall to 434%, when compared to the strength of the cracked wall, but also largely increased the ductility capacity of the wall.

- NSM-TS strengthening resulted in a moderate flexural strength increase for the wall having a large as-built first cracking strength (143% when compared to the strength of the as-built wall) but the subsequent rapid strength degradation was avoided, allowing the strengthened wall to perform in a highly ductile manner.

- For the wall having NSM-TS installed on one face only an asymmetric flexural strength increase was observed when subjected to a reversed cyclic loading, with the flexural strength increase being 300% when the NSM-TS acted in tension and 125% in the reverse direction when the NSM-TS acted in compression.

5. Acknowledgments

The Higher Education Commission of Pakistan provided funding for the doctoral studies of the first author. Financial support for the testing reported herein was provided by the New Zealand Foundation for Research Science and Technology. Helifix Australia supplied the strengthening materials. Hossein Derakhshan, Dmytro Dizhur, Ronald Lumantarna and Tek Goon Ang are thanked for their help with the testing program. Win Clark and John Morrison are thanked for providing the in-situ testing opportunity. Eric Thomas is thanked for providing the photographs of the NSM-TS application.

Tables

Table 1. Masonry material properties

Test series	f'_b (CoV) MPa	MOR (CoV) MPa	E_b (CoV) GPa	f'_j (CoV) MPa	f'_m (CoV) MPa	E_m (CoV) GPa	f_r (CoV) MPa	τ (CoV) MPa
1	8.8 (0.19)	-	-	3.3 (0.37)	3.2 (0.19)	0.4 (0.22)	0.04 (0.50)	0.09
2	18.8 (0.33)	3.0 (0.52)	5.9 (0.44)	0.7 (0.22)	5.6 (0.34)	1.7 (0.49)	0.08 (0.66)	0.10

Where: CoV = coefficient of variation; f'_b = brick compressive strength; MOR = brick modulus of rupture; E_b = brick modulus of elasticity; f'_j = mortar compressive strength; f'_m = masonry compressive strength; E_m = masonry elastic modulus; f_r = masonry flexural bond strength; and τ = masonry diagonal shear strength.

Table 2. Indicative strengthening material properties

Twisted stainless steel bars (ASTM Grade 316)					
D	**A_s**	**f_y**	**f_u**	**f_s**	**E_s**
mm	**mm^2**	**MPa**	**MPa**	**MPa**	**GPa**
6	7.1	1110	1206	679	168
10	14.8	1104	1163	476	168
Thixotropic injectable cementitious grout					
Grout	**Ex_u**	**f'_{2g}**	**f'_{7g}**	**f'_{21g}**	**f'_{28g}**
type	**%**	**MPa**	**MPa**	**MPa**	**MPa**
Cementitious	0.15	15.0	25.0	40.0	45.0

Where: D = outer diameter of TS bar; A_s = effective cross sectional area of TS bar; f_y = 2% proof tensile strength of TS bar; f_u = ultimate tensile strength of TS bar; f_s = averaged shear strength of TS bar; E_s = modulus of elasticity of TS bar; Ex_u = unrestrained expansion when fully cured; and f'_{ng} = strengthening grout compressive strength after n days.

Table 3. Test wall specifications

Test series	Test wall	Wall dimensions					NSM-TS strengthening details					
		H mm	B mm	T mm	t_{pt} mm	t_{pc} mm	D mm	w mm	d mm	No. of NSM cut slots	NSM-TS pattern	S_T mm
1	ABO-1	3325	1200	155	10[a]	20[b]	-	-	-	-	-	-
1	ABO-2	2640	1200	240	25[b]	18[b]	-	-	-	-	-	-
2	ABO-3	3760	1200	220	-	-	-	-	-	-	-	-
1	TSO-4[+]	3325	1200	155	10[a]	20[b]	6	10	30	2	V	600
1	TSO-5	2640	1200	240	25[b]	18[b]	10	14	30	1	V	1200
2	TSO-6	3760	1200	220	-	-	6	10	30	2	V	600

Where: H = test wall height; B = test wall length; T = total test wall thickness; t_{pt} = thickness of plaster on tension face; t_{pc} = thickness of plaster on compression face; D = outer diameter of TS bar; w = width of NSM-TS cut slot; d = depth of NSM-TS cut slot; V = vertically oriented NSM-TS bars; and S_T = centre to centre spacing of NSM-TS bars

[+]retested after repairing wall ABO-1

[a]strong cement based mortar

[b]low strength horse hair reinforced hydraulic mortar

Table 4. Test results

Test series	Test wall	V_c kN	M_c kN.m	V_u kN	M_u kN.m	V_u/V_o Ratio	Δ_c mm	Δ_y mm	Δ_u mm	θ_u %	μ ratio	K_i kN/mm
1	ABO-1	0.40	0.13	0.80	0.26	1.00	-	3.00	62.69	2.37	20.90	0.27
1	ABO-2	4.09	1.66	8.17	3.32	1.00	1.12	2.24	11.12	0.34	4.96	3.65
1	ABO-3	1.69	0.79	3.64	1.71	1.00	1.90	3.79	56.19	1.49	14.83	0.89
2	TSO-4	1.74	0.57	3.47	1.15	4.34	-	18.80	61.12	2.32	3.25	0.19
2	TSO-5	5.85	2.38	11.70	4.75	1.43	0.69	1.38	84.03	2.59	60.89	8.48
2	TSO-6	5.92	2.78	10.91	5.13	3.00	4.44	8.88	77.83	2.07	8.76	1.33
2	TSO-6*	2.18	1.02	4.35	2.04	1.25	1.74	3.48	63.67	1.69	18.30	1.25

Where: V_c = measured lateral force at first cracking limit state; M_c = measured analogous moment at first cracking limit state; Δ_y = effective yield displacement corresponding to extrapolation of the first cracking limit state when considering a bi-linear elasto-plastic system; V_u = maximum measured lateral force; M_u = maximum measured analogous moment; Δ_u = measured displacement at ultimate strength limit state; V_o = ultimate strength of as-built tested wall; θ_u = measured drift at ultimate strength limit state; μ = pseudo-ductility; and K_i= initial wall stiffness.

*'results of test wall in the reverse direction when NSM-TS acted in compression

Figures

(a) 270 Broadway street, Auckland (NZ)

(b) corroded wall ties (left) and newly installed TS ties (right)

(c) bed joint insertion of TS bars

(d) closer view of NSM-TS bars

Figure 1. NSM-TS strengthening application to an actual building

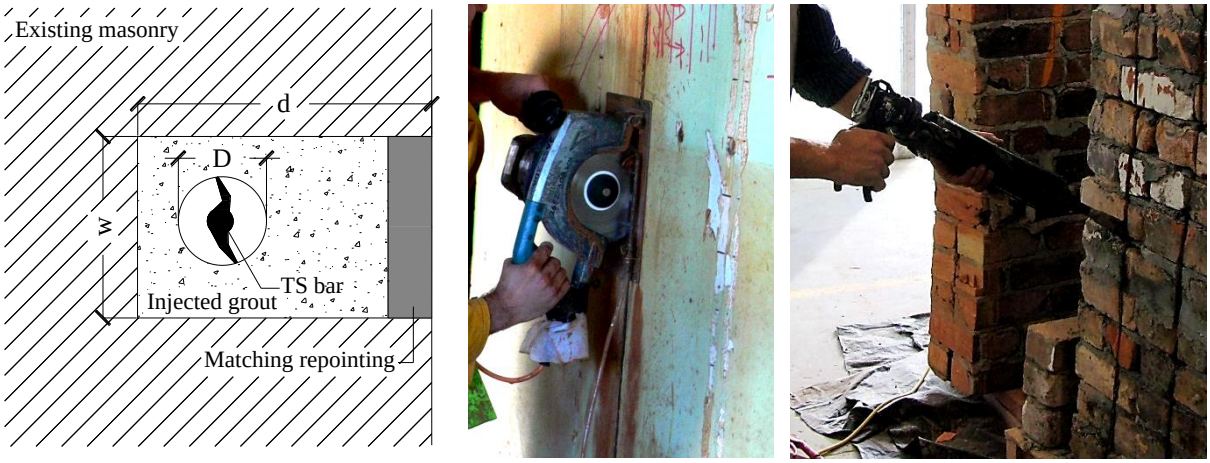

(a) typical NSM-TS details (refer Table 3 for values and definition of symbols)

(b) cutting slots

(c) grout injection

Figure 2. Typical NSM-TS details and application procedure

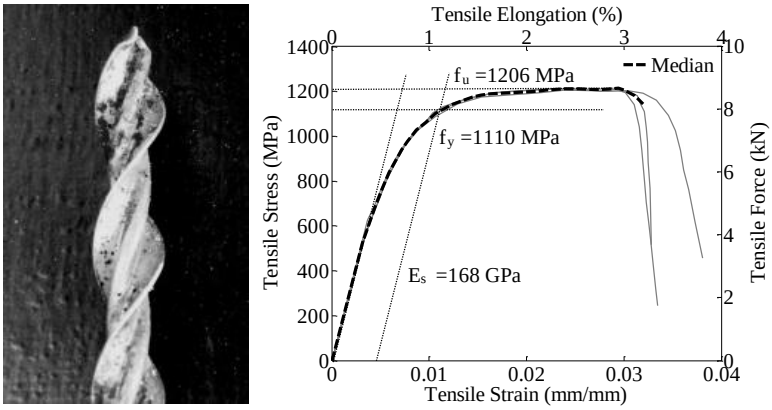

(a) bar geometry (b) stress-strain behaviour

Figure 3. Twisted steel bar details

(a) photograph of Avon house

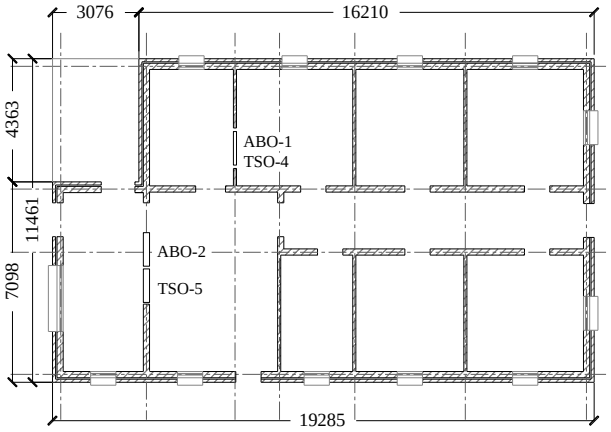

(b) location of test walls inside Avon house

Figure 4. Location of series 1 test walls

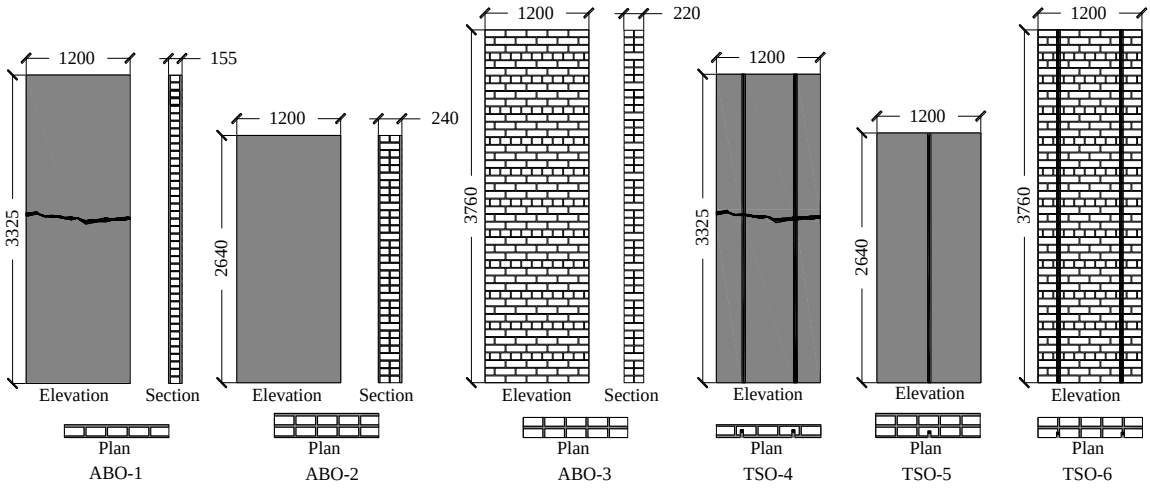

Figure 5. Test wall specifications

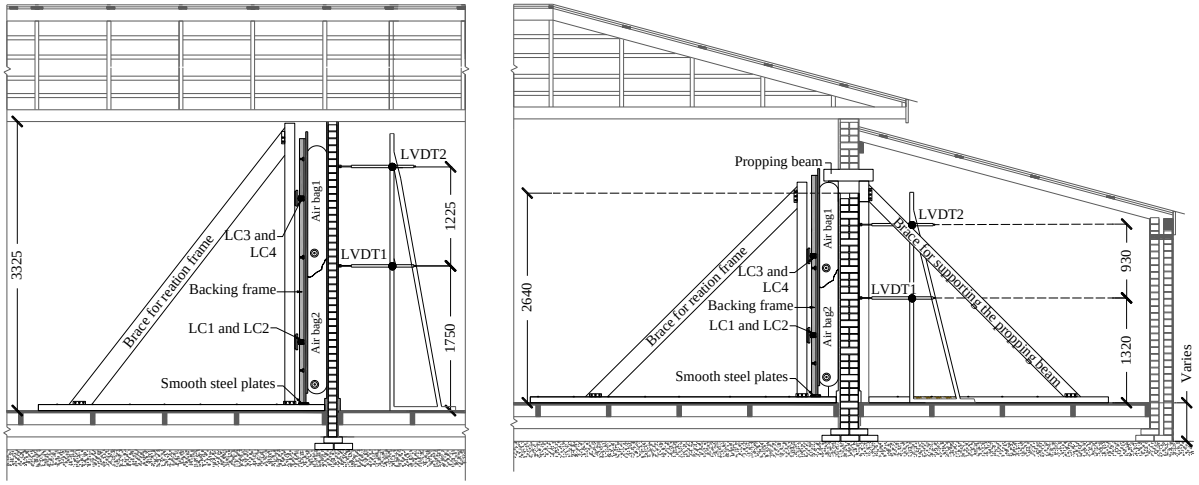

(a) ABO-1 and STO-4 (b) ABO-2 and STO-5

Figure 6. Series 1 testing setup (in-situ testing)

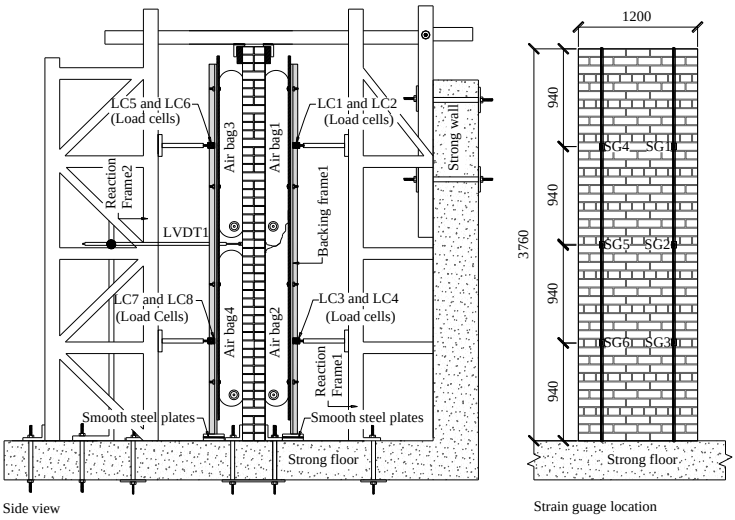

Figure 7. Series 2 testing setup (laboratory based testing)

(a) ABO-1 and TSO-4

(b) ABO-2 and TSO-5

(c) ABO-3 and TSO-6

Figure 8. Photographs of test walls ready to be tested

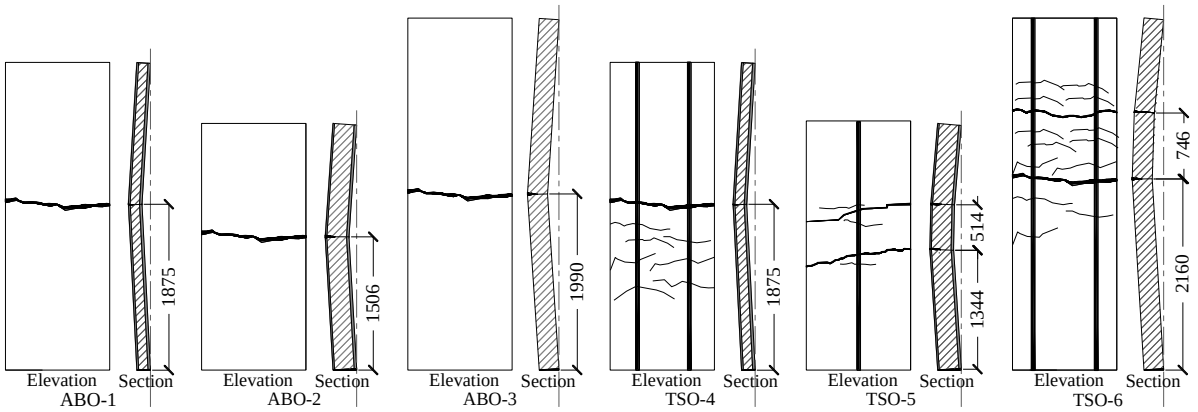

Figure 9. Damage patterns

(a) mortar deterioration (b) cracking through bricks (c) local bending of a NSM-TS bar

Figure 10. Photographs of cracked wall sections

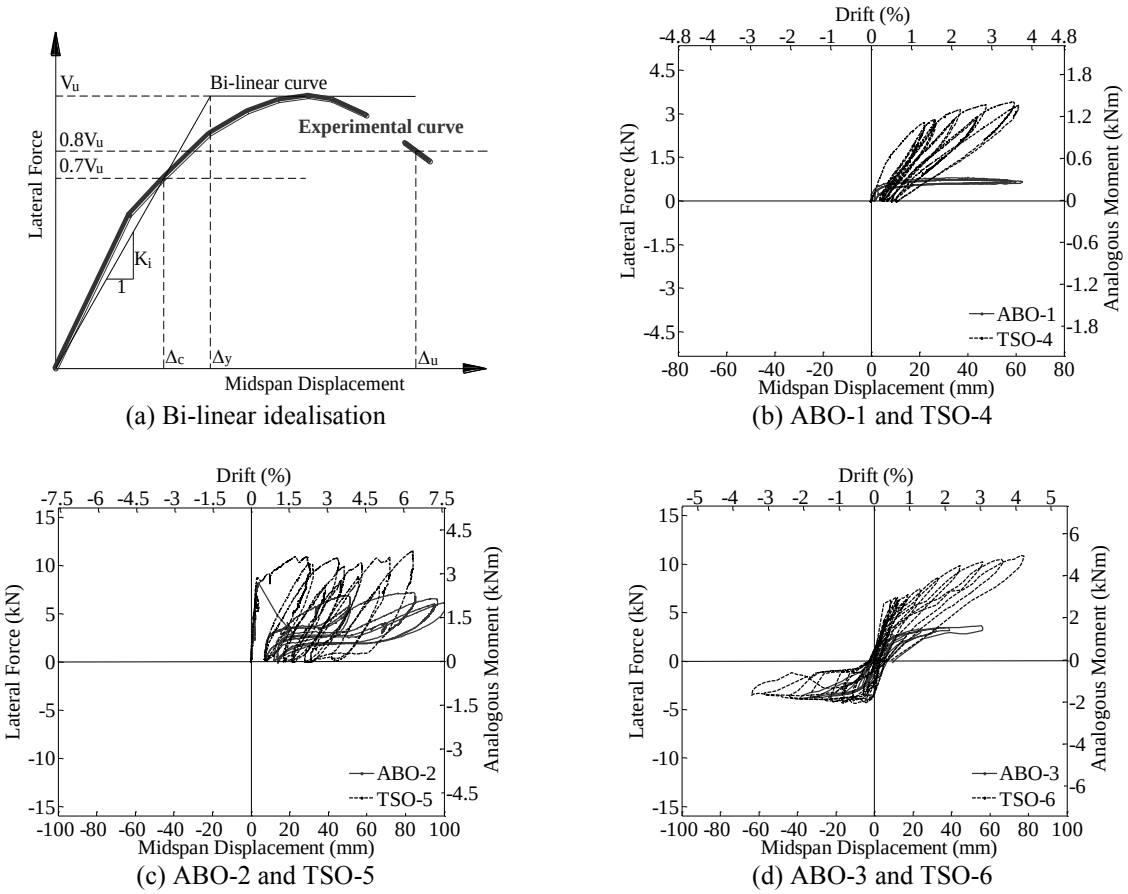

(a) Bi-linear idealisation

(b) ABO-1 and TSO-4

(c) ABO-2 and TSO-5

(d) ABO-3 and TSO-6

Figure 11. Force-displacement curves

6. References

[1] Ingham JM, Griffith MC. The performance of unreinforced masonry buildings in the 2010/2011 Canterbury earthquake swarm. Christchurch, New Zealand: Canterbury Earthquakes Royal Commission; 2011. Available from: http://canterbury.royalcommission.govt.nz/

[2] Dizhur D, Ismail N, Knox C, Lumantarna R, Ingham JM. Performance of unreinforced and retrofitted masonry buildings during the 2010 Darfield earthquake. Bulletin of the New Zealand Society for Earthquake Engineering. 2010;43(4):321-39.

[3] Ingham JM, Biggs DT, Moon LM. How did unreinforced masonry buildings perform in the February 2011 Christchurch earthquake? The Structural Engineer. 2011;89(6):14-8.

[4] Ingham JM, Griffith M. Performance of unreinforced masonry buildings during the 2010 Darfield (Christchurch, NZ) earthquake. Australian Journal of Structural Engineering. 2010;11(3):207-24.

[5] Štepánek P, Czempiel J. Additional reinforcement in the masonry of historical buildings tests, numerical analysis, practical application. In: Lourenço PB, Roca P, editors. 3rd International Seminar on Historical Constructions. Guimarães, Portugal: University of Minho; 2011. p. 1013-22.

[6] Ismail N, Petersen RB, Masia MJ, Ingham JM. Diagonal shear behaviour of unreinforced masonry wallettes strengthened using twisted steel bars. Construction and Building Materials. 2011;25(12):4386–93.

[7] Zlámal M, Štěpánek P. Additional strengthening of masonry vaulted structures by nonprestressed reinforcement. Architecture Civil Engineering Environment. 2009;2(3):85-90.

[8] Chen Y, Ashour AF, Garrity SW. Modified four-hinge mechanism analysis for masonry arches strengthened with near-surface reinforcement. Engineering Structures. 2007;29(8):1864–71.

[9] Garrity SW. The rehabilitation of short span masonry arch highway bridges using near-surface reinforcement. Proceedings of 8th International Conference on Short and Medium Span Bridges. Niagara Falls, Canada; 2010. 075.1-11.

[10] Turco V, Secondin S, Morbin A, Valluzzi MR, Modena C. Flexural and shear strengthening of un-reinforced masonry with FRP bars. Composites Science and Technology. 2006;66(2):289–96.

[11] Willis CR, Seracino R, Griffith MC. Out-of-plane strength of brick masonry retrofitted with horizontal NSM CFRP strips. Engineering Structures. 2010;32(2):547–55.

[12] Valluzzi MR, Binda L, Modena C. Mechanical behaviour of historic masonry structures strengthened by bed joints structural repointing. Construction and Building Materials. 2005;19(1):63–73.

[13] Modena C, Valluzzi MR. Repair techniques for creep and long-term damage of massive structures. In: Carlos B, editor. Structural studies, repairs and maintenance of Heritage Architecture VIII. Southampton, UK: Wessex Institute of Technology Press; 2003. p. 141–50.

[14] Lumantarna R. Characterisation of materials in URM buildings in New Zealand [PhD Thesis]. Auckland, New Zealand: University of Auckland; 2012.

[15] ASTM Committee C1072-10. Standard test method for measurement of masonry flexural bond strength. West Conshohoken, USA: American Society for Testing and Materials International; 2010.

[16] AS/NZS Committee 4456. Masonry Units, Segmental Pavers and Flags - Methods of Test. Sydney, Australia: Standards Australia; 2003.

[17] ASTM Committee C109-11. Standard test method for compressive strength of hydraulic cement mortars. West Conshohoken, USA: American Society for Testing and Materials International; 2011.

[18] ASTM Committee C67-11. Standard test methods for sampling and testing brick and structural clay tile. West Conshohoken, USA: American Society for Testing and Materials International; 2011.

[19] ASTM Committee C1314-11. Standard test method for compressive strength of masonry prisms. West Conshohoken, USA: American Society for Testing and Materials International; 2011.

[20] ASTM Committee E519-10. Standard test method for diagonal tension (shear) in masonry assemblages. West Conshohoken, USA: American Society for Testing and Materials International; 2010.

[21] Derakhshan H. Seismic assessment of out-of-plane loaded unreinforced masonry walls [PhD Thesis]. Auckland, New Zealand: University of Auckland; 2011.

[22] Eurocode 8: Design of structures for earthquake resistance. Brussels, Belgium: Comite Europeen de Normalisation (European Committee for Standardization); 2005.

[23] ASCE/SEI 41-06: Seismic rehabilitation of existing buildings. Reston, USA: American Society of Civil Engineers; 2006.